Mono- and Di-nuclear Nickel(II) Complexes with Schiff Bases derived from 4-Substituted 2,6-Diformylphenol and 7-Amino-4-methyl-5-azahept-3-en-2-one; Crystal and Molecular Structure of [4-Chloro-2,6-bis(4-methyl-2-oxo-5,8-diazanona-3,8-dienyl)phenolato(3−)]dinickel(II) Bromide Hemihydrate†

Marek Kwiatkowski,* Edmund Kwiatkowski, and Aleksandra Olechnowicz
Institute of Chemistry, University of Gdańsk, Sobieskiego 18, 80-952 Gdańsk, Poland
Douglas M. Ho and Edward Deutsch
Biomedical Chemistry Research Center and Department of Chemistry, University of Cincinnati, Cincinnati, Ohio 45221-0172, U.S.A.

The reaction of 4-chloro- or 4-methyl-2,6-diformylphenol with 7-amino-4-methyl-5-azahept-3-en-2-one leads to either quadridentate mononucleating or heptadentate binucleating Schiff-base ligands, depending on the reaction conditions. Nickel complexes with both types of ligands have been obtained and characterized by i.r., u.v.–visible, n.m.r., and mass spectrometry. An interesting example of impeded pseudo-rotation of a five-membered chelate ring in dinuclear nickel complexes is observed. The single-crystal *X*-ray structure of [4-chloro-2,6-bis(4-methyl-2-oxo-5,8-diazanona-3,8-dienyl)phenolato(3−)]dinickel(II) bromide hemihydrate has been determined. It consists of a dinuclear complex cation of twisted bifurcated shape and a bromide anion, with a half-equivalent of water incorporated into the crystal lattice. Crystallographic data: space group $C2/c$ (no. 15), a = 22.082(4), b = 11.5, c = 22.368(4) Å, β = 118.61(1)°, R and R' 0.0380 and 0.0318, respectively.

The condensation of a free primary amino group in 7-amino-4-methyl-5-azahept-3-en-2-one (**2**) with the carbonyl group in *ortho*-substituted aromatic carbonyl compounds (**1**) provides an excellent synthetic route to the unsymmetrical quadridentate Schiff-base ligands (**3**) (Scheme 1) and their transition-metal complexes.[1–3] Our recent studies[3] have revealed that the formation of the unsymmetrical ligand (**3**) is catalyzed by the intramolecular hydrogen bonding between the hydrogen atom on the X substituent (X = OH, NH_2, or NHOCMe) and the carbonyl oxygen atom in (**1**) and depends on the acidity of this hydrogen atom.

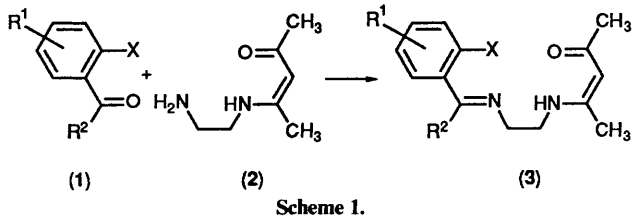

(1) (2) (3)

Scheme 1.

Aromatic hydroxydialdehydes of the type (**4**) can react with two molecules of (**2**) according to Scheme 2. The first step of this reaction should proceed with ease due to the strong intramolecular hydrogen bond between the acidic phenolic hydrogen and carbonyl oxygen atoms in (**4**). However the condensation with the second molecule of (**2**) should be more difficult, since the hydrogen bonding to the more basic imino nitrogen atom is preferred in (**5**), and the intramolecular catalysis is less effective. This difference in reactivity of the two carbonyl groups in (**4**) offers the possibility of the preparation of either mononucleating ligands of the type (**5**), or dinucleating ligands of the type (**6**), depending on the reaction conditions employed. Indeed, we have found that at room temperature this reaction stops at the stage of the mononucleating ligands (**5**), whereas at elevated temperature the dinucleating ligands (**6**) are formed. In this paper we report the preparation of two new

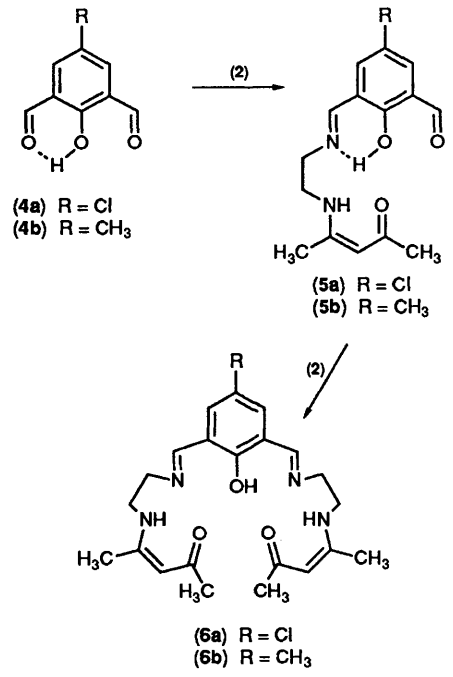

(**4a**) R = Cl
(**4b**) R = CH_3

(**5a**) R = Cl
(**5b**) R = CH_3

(**6a**) R = Cl
(**6b**) R = CH_3

Scheme 2.

mononucleating ligands (**5a**) and (**5b**) and two new binucleating Schiff-base ligands (**6a**) and (**6b**) derived from 4-chloro- and 4-methyl-2,6-diformylphenol (**4a**) and (**4b**). The ligands have been used for the preparation of mono- and di-nuclear nickel complexes, which have been characterized by spectroscopic

† *Supplementary data available:* see Instructions for Authors, *J. Chem. Soc., Dalton Trans.*, 1990, Issue 1, pp. xix—xxii.

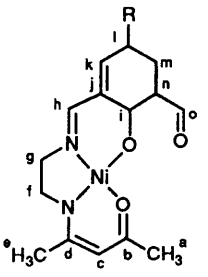

(7a) R = Cl
(7b) R = CH_3

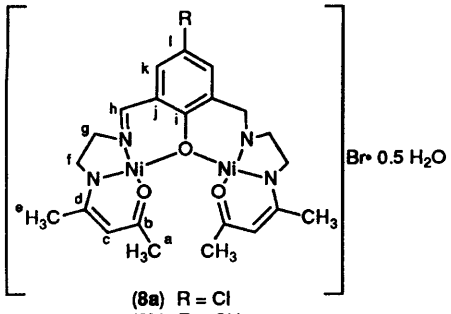

(8a) R = Cl
(8b) R = CH_3

techniques. The single-crystal *X*-ray structure of one of the dinuclear complexes, [4-chloro-2,6-bis(4-methyl-2-oxo-5,8-diazanona-3,8-dienyl)phenolato(3−)]dinickel(II) bromide hemihydrate has been determined.

Results and Discussion

The mononucleating ligands 4-chloro-2-formyl-6-(4-methyl-2-oxo-5,8-diazanona-3,8-dienyl)phenol (**5a**) and 2-formyl-4-methyl-6-(4-methyl-2-oxo-5,8-diazanona-3,8-dienyl)phenol (**5b**) were obtained by the reaction of the appropriate dialdehyde (**4**) with an equimolar amount of the precursor (**2**) (the mono-condensation product of pentane-2,4-dione and 1,2-diaminoethane) at room temperature. When the reaction was carried out in refluxing dichloromethane and 2 mol of (**2**) were used per mol of the dialdehyde two new binucleating ligands 4-chloro-2,6-bis(4-methyl-2-oxo-5,8-diazanona-3,8-dienyl)phenol (**6a**) and 4-methyl-2,6-bis(4-methyl-2-oxo-5,8-diazanona-3,8-dienyl)phenol (**6b**) were obtained. Since the full characterization of the ligands was beyond the scope of this work their identity was confirmed by observation of the molecular ions in their f.d. (Field Desorption) mass spectra and the crude ligands were used for the preparation of nickel complexes.

The nickel complexes described in this paper are diamagnetic, crystalline, red-brown (**7a**) and (**7b**) or dark brown (**8a**) and (**8b**) solids. The mononuclear complexes (**7**) are neutral, *i.e.* the charge on nickel is entirely neutralized by the doubly deprotonated Schiff-base molecule. The dinuclear compounds (**8**) are composed of an unipositive complex cation incorporating two nickel ions bound by a triply deprotonated heptadentate Schiff base, and unco-ordinated bromide ion acting as counter anion. In addition one molecule of water per two complex cations is incorporated in the crystal lattice.

F.a.b. (fast atom bombardment) mass spectra of the nickel complexes provide direct proof of their composition. In the spectra of the mononuclear nickel complexes the peaks corresponding to $[M + H]^+$ ions are present at m/z = 365 and 345 for (**7a**) and (**7b**), respectively. Characteristic peaks of $[M - 28]^+$ species formed by the loss of CO from the unco-ordinated aldehyde group are also observed. Complexes (**8**) are not volatile enough to give an ion pair peak in their f.a.b. mass spectra, however the peaks corresponding to the complex dinuclear cation M^+ at m/z = 545 and 525 for (**8a**) and (**8b**), respectively, are quite intense. Also the fragmentation ions $[M - 125]^+$ formed by the loss of $CH_3COCH(CH_3)$-$CNCH_2CH_2$ are observed in the spectra of both dinuclear complexes. Due to the natural abundance of nickel and chlorine isotopes, the peaks discussed above have the appearance of clusters of peaks rather than single peaks.

In the i.r. spectra of all the nickel complexes (Table 1) a group of strong bands corresponding to C=O, C=N, and C=C stretching vibrations within the co-ordinated ligand molecule is observed in the 1 500—1 650 cm^{-1} region. An additional strong C=O stretching band of the unco-ordinated aldehyde group is present at 1 670 and 1 655 cm^{-1} in the spectra of mononuclear complexes (**7a**) and (**7b**), respectively. Dinuclear complexes (**8**) exhibit broad absorption bands of medium intensity in the 3 100—3 600 cm^{-1} region due to the water molecules incorporated into the crystal lattice.

Two or three intense absorption bands are present in the u.v. spectra of the nickel complexes (Table 1), with shoulders of *d–d* transitions extending into the visible region. This pattern and an absence of lower-energy *d–d* transitions is indicative of square-planar geometry around the individual nickel ions.[4] The intense u.v. bands result from transitions within the ligand and/or metal-to-ligand charge-transfer transitions.

Proton n.m.r. data for the nickel complexes are collected in Table 1. The spectra of mononuclear complexes (**7**) resemble generally those of similar compounds of type (**3**) reported earlier[1,3] and their interpretation is quite straightforward. The conspicuous feature of these spectra is the presence of a singlet at δ *ca.* 10.4 corresponding to the proton of the unco-ordinated aldehyde group. The spectra of dinuclear complexes (**8**) indicate the considerable degree of symmetry of the complex cation in solution, since the corresponding protons in the two halves of the complex seem to be magnetically equivalent (in the solid state the C_2 symmetry is distorted to some extent by the slight 'out-of-axis' bending of the benzene ring, see below). These spectra are similar in general appearance to those of the corresponding mononuclear complexes though obviously the signal of the aldehyde proton is no longer present and the relative intensities of the signals are different.

Some other differences between the ^1H n.m.r. spectra of mono- and di-nuclear nickel complexes are also of note. The most striking is in the resonance of so-called 'ethylene bridge', *i.e.* adjacent methylene groups f and g. In the spectra of mononuclear nickel complexes (**7**) this resonance has the form of two triplets [Figure 1(*a*)], characteristic for two groups of two magnetically equivalent protons A_2X_2 coupled together with a single coupling constant J_{AX} [in this case $J(H^fH^g)$ = 6.6 Hz for both mononuclear complexes]. The equivalence of the protons within each methylene group is achieved by fast interconversion between two alternative conformations of the five-membered chelate ring. A long-range coupling between methylene protons g and methine proton h results in additional splitting of the lower-field triplet [for (**7a**) the coupling constant $J(H^gH^h)$ is *ca.* 1.1 Hz]. In the spectra of the dinuclear complexes the signals of the ethylene bridge are more complex and can be approximated as an ABX_2 pattern characterized by the three coupling constants J_{AB}, J_{AX}, and J_{BX} [Figure 1(*b*)]. The two protons g and g′ on the methylene carbon atoms linked to the imino nitrogen atoms are no longer magnetically equivalent, whilst the two protons f of the adjacent methylene carbon atoms are equivalent. This phenomenon presumably arises from the constraints imposed upon the ethylene bridges by their linkage to independently planar moieties which are not themselves coplanar. The structural analysis for complex (**8a**) shows that both portions of the chelate which encompass the aromatic hydroxydialdimine moiety, and the ketoenamine portions, are

Table 1. Spectroscopic data for the nickel complexes

Complex	I.r.[a] ν/cm^{-1}	U.v.–visible[b] $\lambda_{max.}$/nm (log ε)	N.m.r. (δ) ^1H[c]	N.m.r. (δ) ^{13}C
(**7a**)	1 520s	243 (4.68)	1.921 (s), 1.931 (s) ($H^{a,e}$), 3.091 (t)	24.20 ($C^{a,e}$), 51.38 (C^f), 60.65 (C^g),
	1 545s	345 (3.84)	(H^f), 3.426 (t) (H^g),[d] 5.021 (s) (H^c),	100.17 (C^c), 119.45, 124.50, 132.98,
	1 585s	365 (sh)	7,250 (d) (H^k), 7.449 (s) (H^h), 7.729	137.44 (C^{i-n}), 160.09 (C^d), 165.53
	1 630s	426 (3.40)	(d) (H^m), 10.390 (s) (H^o), $J(H^fH^g)$	(C^h), 189.86 (C^o)
	1 670s	455 (3.37)	6.6 Hz	
(**7b**)	1 515s	241 (4.70)	1.921 (s) ($H^{a,e}$), 2.200 (s) (R), 3.088 (t)	19.80 (R), 21.39, 24.20 ($C^{a,e}$), 51.44
	1 540s	350 (3.92)	(H^f), 3.407 (t) (H^g), 4.990 (s) (H^c),	(C^f), 60.37 (C^g), 99.98 (C^c), 123.05,
	1 585s	452 (3.74)	7.075 (d) (H^k), 7.411 (s) (H^h), 7.624	123.34, 126.05, 139.26 (C^{i-n}), 160.72
	1 632s	570 (sh)	(d) (H^m), 10.454 (s) (H^o), $J(H^fH^g)$	(C^d), 165.40 (C^h), 177.27 (C^b), 191.16
	1 655s		6.6, $J(H^kH^m)$ 2.4 Hz	(C^o)
(**8a**)	1 510s	237 (4.75)	1.971 (s), 2.232 (s) ($H^{a,e}$), 2.934 (d)	21.22, 23.65 ($C^{a,e}$), 51.01 (C^f), 60.33
	1 562s	345 (4.12)	(H^f), 3.390 (q), 3.736 (d) ($H^{g,g'}$),[e]	(C^g), 100.24 (C^c), 125.34, 137.15
	1 582s	446 (sh)	5.061 (s) (H^c), 7.693 (s) (H^k), 8.539	(C^{i-l}), 163.19, 165.69 ($C^{d,h}$), 176.24
	1 640s	575 (sh)	(s) (H^h), $J(H^gH^{g'})$ 12, $J(H^fH^g)$ 3,	(C^b)
	3 440m (br)		$J(H^fH^{g'})$ 10 Hz	
(**8b**)	1 515s	235 (4.68)	1.955 (s), 2.216 (s) ($H^{a,e}$), 2.362 (s)	19.97 (R), 21.22, 23.65 ($C^{a,e}$), 51.08
	1 570s	345 (4.08)	(R), 2.921 (m) (H^f), 3.356 (q), 3.678 (d)	(C^f), 60.28 (C^g), 100.24 (C^c), 123.88,
	1 615s	580 (sh)	($H^{g,g'}$), 3.549 (br) (H_2O), 5.044 (s)	128.93, 138.97, 155.60 (C^{i-l}), 162.62,
	1 642s		(H^c), 7.486 (s) (H^k), 8.239 (s) (H^h),	165.66 ($C^{d,h}$), 176.20 (C^b)
	3 380m (br)		$J(H^gH^{g'})$ 13, $J(H^fH^g)$ 4, $J(H^fH^{g'})$ 11 Hz	

[a] s = Strong, m = medium, and br = broad. [b] sh = Shoulder. [c] s = Singlet, d = doublet, t = triplet, q = quartet, m = multiplet, and br = broad. [d] Additional splitting due to g–h coupling with $J(H^gH^h)$ 1.1 Hz. [e] Additional splitting due to g–h coupling with $J(H^gH^h)$ 2 Hz.

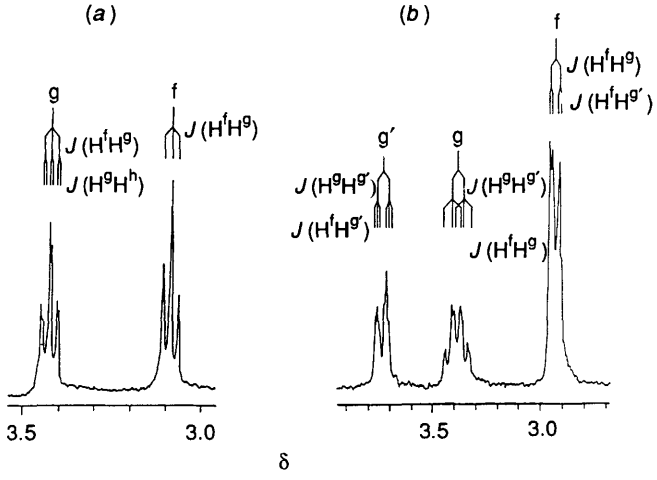

Figure 1. Proton n.m.r. resonances of methylene groups f and g in (*a*) mononuclear nickel complex (**7a**), (*b*) dinuclear nickel complex (**8a**). The additional g–h coupling, visible in the signals g and g′ in (*b*), was omitted in the coupling scheme for clarity. Values of chemical shifts and coupling constants are given in Table 1.

independently planar. However, the two ketoenamine portions cannot be coplanar because of the steric interactions between carbonyl oxygen atoms b and methyl groups a in such a hypothetical coplanar structure. As a result the molecule assumes a twisted bifurcated shape with terminal parts pushed apart by two interacting carbonyl oxygen atoms b, located at a distance almost equal (0.01 Å shorter) to the sum of two van der Waals radii (see below). The model studies show that the dinuclear complex cation forms a fairly rigid structure, and that flexing to the alternate overall conformation is virtually impossible as it would require a severely strained intermediate to let the terminal methyl groups a pass each other. This gives a strong indication that the general shape of the chelate in solution and in the solid state is quite similar. Furthermore, the model reveals that pseudorotation of the ethylene bridges from the staggered conformation present in the crystal structure to the alternative staggered one is feasible, though it inevitably moves the carbonyl oxygen atoms b closer to each other, increasing the strain within the molecule even more. Thus the flexibility of the ethylene bridges is substantially restricted. Proton n.m.r. results indicate that motion of the methylene groups g, joined to the aromatic portion of the molecule, is restricted with respect to the local centres of magnetic anisotropy more than is motion of the adjacent methylene group f. *X*-Ray structural analysis shows that the two methylene protons g and g′ differ significantly in their distances from the centre of the adjacent C=N bond which is the closest centre of magnetic anisotropy [2.15 and 2.37 Å, respectively, from the calculated hydrogen positions on C(6) and C(17) in (**8a**), see below]. Thus it is not unreasonable that the restricted flexibility of the ethylene bridge could force these two protons into magnetically non-equivalent environments, even in solution. Close inspection of the resonances arising from the ethylene bridges reveals additional splitting of the g and g′ resonances by long-range coupling to proton h of the adjacent methine group [$J(H^gH^h)$ *ca.* 2 Hz]. The signal for proton h is broadened by this coupling, but in this experiment it is not resolved into its components,.

Another conspicuous difference between the ^1H n.m.r. spectra of the mono- and di-nuclear nickel complexes exists in the chemical shifts of the corresponding protons. For example for dinuclear compounds (**8**) the resonances of methine proton h and aromatic proton k are shifted downfield by *ca.* 1 and 0.4 p.p.m., respectively, from the corresponding resonances in the spectra of mononuclear (**7**). Also methyl resonances a and e are separated by *ca.* 0.26 p.p.m. for (**8**) whereas for (**7**) they appear very close to each other (separation 0.01 p.p.m. or less). All these chemical shift differences result probably from the twisted conformation of the dinuclear cation as compared to the essentially planar structure of the mononuclear complex.

The unambiguous assignment of all resonances in ^{13}C n.m.r. spectra of the nickel complexes (Table 1) is not possible, since some of them are not observed due to their low intensity and low solubility of the complexes, which consequently results in a low signal-to-noise ratio. However the tentative assignment of most of them is quite straightforward (Table 1). In the spectra of the

Table 2. Fractional atomic co-ordinates ($\times 10^4$) for the dinuclear nickel complex (**8a**)

Atom	*x*	*y*	*z*	Atom	*x*	*y*	*z*
Br	8 596(1)	−2 717(1)	6 582(1)	C(6)	4 537(4)	2 497(9)	5 459(5)
Ni(1)	5 623(1)	1 623(1)	5 289(1)	C(7)	5 199(5)	3 074(8)	5 995(5)
Ni(2)	6 812(1)	1 508(1)	4 906(1)	C(8)	6 286(5)	2 213(8)	6 667(5)
Cl	8 534(1)	337(2)	8 479(1)	C(9)	6 899(4)	1 548(8)	6 816(5)
O(1)	5 515(3)	769(5)	4 551(3)	C(10)	7 362(4)	1 293(8)	7 480(5)
O(2)	6 598(3)	1 459(5)	5 639(3)	C(11)	7 954(5)	683(8)	7 640(5)
O(3)	6 247(3)	2 776(5)	4 600(3)	C(12)	8 094(4)	311(8)	7 133(5)
O(4)	5 000(*)	6 076(11)	2 500(*)	C(13)	7 652(5)	575(8)	6 457(5)
N(1)	4 702(3)	1 930(6)	4 966(4)	C(14)	7 041(4)	1 199(7)	6 288(5)
N(2)	5 772(4)	2 342(6)	6 085(4)	C(15)	7 805(4)	113(8)	5 936(6)
N(3)	7 466(4)	367(6)	5 304(4)	C(16)	7 607(5)	−263(9)	4 809(5)
N(4)	6 924(4)	1 351(7)	4 151(4)	C(17)	7 496(5)	559(9)	4 246(5)
C(1)	5 014(5)	58(9)	3 425(5)	C(18)	6 634(5)	1 519(10)	2 957(5)
C(2)	4 942(5)	624(8)	3 999(5)	C(19)	6 545(6)	1 846(9)	3 571(6)
C(3)	4 311(5)	974(8)	3 905(5)	C(20)	6 033(5)	2 664(9)	3 456(5)
C(4)	4 194(4)	1 562(8)	4 383(5)	C(21)	5 919(5)	3 078(8)	3 972(6)
C(5)	3 460(4)	1 790(9)	4 211(5)	C(22)	5 377(5)	4 009(9)	3 819(5)

* Parameter constrained in keeping with the space-group symmetry requirements; Wyckoff 4e.

Table 3. Bond distances (Å) for non-hydrogen atoms in the dinuclear nickel complex (**8a**)

Ni(1)–O(1)	1.835(6)	O(2)–C(14)	1.339(9)	N(4)–C(19)	1.292(11)	C(11)–C(12)	1.376(11)
Ni(1)–O(2)	1.916(5)	O(3)–C(21)	1.281(10)	C(1)–C(2)	1.514(11)	C(12)–C(13)	1.386(11)
Ni(1)–N(1)	1.839(7)	N(1)–C(4)	1.318(10)	C(2)–C(3)	1.366(11)	C(13)–C(14)	1.410(10)
Ni(1)–N(2)	1.846(7)	N(1)–C(6)	1.469(10)	C(3)–C(4)	1.392(11)	C(13)–C(15)	1.461(11)
Ni(2)–O(2)	1.912(5)	N(2)–C(7)	1.451(10)	C(4)–C(5)	1.498(10)	C(16)–C(17)	1.499(11)
Ni(2)–O(3)	1.827(6)	N(2)–C(8)	1.261(9)	C(6)–C(7)	1.529(11)	C(18)–C(19)	1.524(11)
Ni(2)–N(3)	1.837(7)	N(3)–C(15)	1.277(10)	C(8)–C(9)	1.447(11)	C(19)–C(20)	1.398(12)
Ni(2)–N(4)	1.829(7)	N(3)–C(16)	1.475(10)	C(9)–C(10)	1.372(10)	C(20)–C(21)	1.380(12)
Cl–C(11)	1.738(9)	N(4)–C(17)	1.488(10)	C(9)–C(14)	1.419(10)	C(21)–C(22)	1.518(11)
O(1)–C(2)	1.287(9)			C(10)–C(11)	1.373(11)		

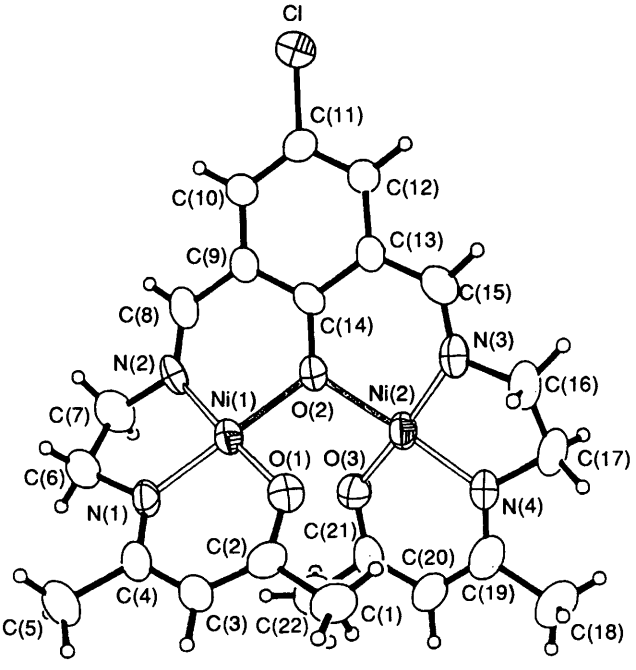

Figure 2. Perspective view of the dinuclear cation in the nickel complex (**8a**) including the atom numbering scheme

mononuclear complexes (**7**) the signal corresponding to the carbonyl carbon atom of the unco-ordinated aldehyde substituent is observed at *ca.* 190 p.p.m. The spectra of dinuclear complexes (**8**) again point to a high degree of symmetry in the complex cation, since no splitting of resonances is observed. It is interesting that, contrary to the proton spectra, ^{13}C chemical shifts of corresponding carbon atoms in the mono- and di-nuclear complexes are almost identical. This once more indicates that the differences in proton chemical shifts of corresponding atoms in complexes (**7**) and (**8**) result from the different conformations of these two types of compounds, rather than from different distributions of electronic density in the molecules.

The crystal structure of the dinuclear nickel complex (**8a**) has been determined. The fractional atomic co-ordinates, selected bond distances, and angles are presented in Tables 2, 3, and 4, respectively. The structure is composed of a 1:1 mixture of dinuclear unipositive cations and bromide anions plus a half equivalent of lattice water molecules. A perspective view of the complex cation is shown in Figure 2.

Each nickel ion is co-ordinated to one oxygen and two nitrogen atoms from the diketodi-imine fragment of the ligand while their fourth co-ordination sites are occupied by a common phenolic oxygen atom with the formation of a Ni–O–Ni bridge. Both nickel ions are in square-planar environments with the mean deviation from the least-squares plane defined by Ni(1), O(1), O(2), N(1), N(2) being 0.0651 Å and from Ni(2), O(2), O(3), N(3), N(4) being 0.1092 Å. The Ni–O and Ni–N distances involving the pentane-2,4-dione moieties differ slightly from one nickel centre to the other with the observed averages being 1.831(4) and 1.834(3) Å, respectively. These average values are close to the lower limits of ranges 1.83—1.87 and 1.83—1.89 Å for Ni–O and Ni–N distances, respectively, normally observed in N_2O_2 square-planar nickel(II) complexes.[5] The Ni(1)–O(2)–Ni(2) bridge is symmetric with the average Ni–O(phenolate)

Table 4. Bond angles (°) for complex (**8a**)

O(2)–Ni(1)–O(1)	87.2(2)	C(21)–O(3)–Ni(2)	123.6(6)	C(4)–C(3)–C(2)	125.2(9)	C(15)–C(13)–C(12)	118.7(8)
N(1)–Ni(1)–O(1)	96.1(3)	C(4)–N(1)–Ni(1)	125.7(6)	C(3)–C(4)–N(1)	122.2(8)	C(15)–C(13)–C(14)	121.9(9)
N(1)–Ni(1)–O(2)	174.5(3)	C(6)–N(1)–Ni(1)	114.6(6)	C(5)–C(4)–N(1)	120.1(9)	C(9)–C(14)–O(2)	120.1(7)
N(2)–Ni(1)–O(1)	174.0(3)	C(6)–N(1)–C(4)	119.0(7)	C(5)–C(4)–C(3)	117.7(9)	C(13)–C(14)–O(2)	120.9(8)
N(2)–Ni(1)–O(2)	90.3(3)	C(7)–N(2)–Ni(1)	112.7(6)	C(7)–C(6)–N(1)	107.1(7)	C(13)–C(14)–C(9)	119.1(8)
N(2)–Ni(1)–N(1)	86.8(3)	C(8)–N(2)–Ni(1)	126.8(6)	C(6)–C(7)–N(2)	107.4(7)	C(13)–C(15)–N(3)	124.3(8)
O(3)–Ni(2)–O(2)	86.6(3)	C(8)–N(2)–C(7)	120.4(8)	C(9)–C(8)–N(2)	125.5(9)	C(17)–C(16)–N(3)	108.1(8)
N(3)–Ni(2)–O(2)	91.3(3)	C(15)–N(3)–Ni(2)	127.5(7)	C(10)–C(9)–C(8)	119.5(9)	C(16)–C(17)–N(4)	107.1(7)
N(3)–Ni(2)–O(3)	172.1(3)	C(16)–N(3)–Ni(2)	112.8(6)	C(14)–C(9)–C(8)	120.9(8)	C(18)–C(19)–N(4)	119.6(10)
N(4)–Ni(2)–O(2)	170.7(3)	C(16)–N(3)–C(15)	119.7(8)	C(14)–C(9)–C(10)	119.5(8)	C(20)–C(19)–N(4)	124.1(9)
N(4)–Ni(2)–O(3)	95.9(3)	C(17)–N(4)–Ni(2)	114.1(6)	C(11)–C(10)–C(9)	121.0(8)	C(20)–C(19)–C(18)	116.3(10)
N(4)–Ni(2)–N(3)	87.4(3)	C(19)–N(4)–Ni(2)	125.1(7)	C(10)–C(11)–Cl	121.0(8)	C(21)–C(20)–C(19)	122.3(9)
C(2)–O(1)–Ni(1)	125.3(6)	C(19)–N(4)–C(17)	120.8(8)	C(12)–C(11)–Cl	118.6(7)	C(20)–C(21)–O(3)	126.2(9)
Ni(2)–O(2)–Ni(1)	109.7(3)	C(1)–C(2)–O(1)	114.5(8)	C(12)–C(11)–C(10)	120.4(9)	C(22)–C(21)–O(3)	114.2(9)
C(14)–O(2)–Ni(1)	124.0(5)	C(3)–C(2)–O(1)	124.8(8)	C(13)–C(12)–C(11)	120.8(8)	C(22)–C(21)–C(20)	119.6(10)
C(14)–O(2)–Ni(2)	125.7(5)	C(3)–C(2)–C(1)	120.6(9)	C(14)–C(13)–C(12)	119.2(8)		

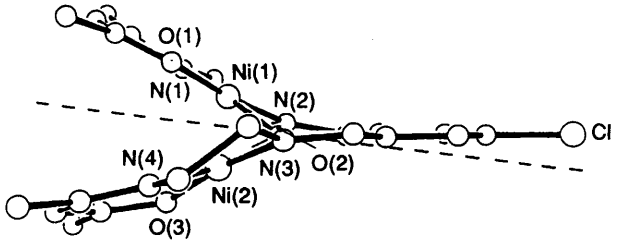

Figure 3. A view of the dinuclear cation in complex (**8a**) showing the slight distortion from C_2 symmetry. A broken line denotes the hypothetical C_2 axis roughly defined by the two nickel-comprising 'halves' of the complex cation

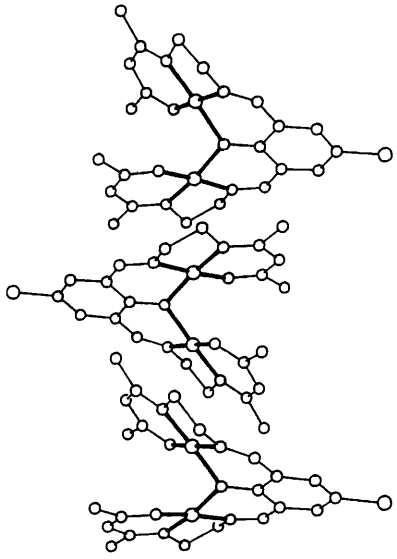

Figure 4. Packing scheme for the dinuclear nickel complex (**8a**)

distance being 1.914(2) Å, the Ni–O–Ni angle 109.7(3)°, and Ni(1) • • • Ni(2) 3.130(1) Å.

The most interesting feature of complex (**8a**) lies in the twist of both nickel co-ordination planes, one against the other, with the dihedral angle $\Phi = 56.6°$, and consequently a bifurcated shape of the complex cation. Such distortion from the totally planar arrangement is caused by the steric interactions between the carbonyl oxygen atoms O(1) and O(3). The non-bonded O(1) • • • O(3) distance is 2.79(1) Å, which is essentially equal to the sum of the oxygen van der Waals radii (2.80 Å). The benzene ring and the adjacent aldimine fragments are all essentially planar with only small out-of-plane deviations. However, the overall structure has no C_2 symmetry since the planar aromatic fragment bends slightly out of the hypothetical C_2 axis roughly defined by two nickel-comprising 'halves' (Figure 3). The local geometries around the nitrogen atoms and carbon atoms C(2)–C(4), C(8)–C(15), and C(19)–C(21) are all planar. The augmented N(2)–C(8)–C(9), N(3)–C(15)–C(13), C(14)–O(2)–Ni(1), and C(14)–O(2)–Ni(2) angles of 125.5(9), 124.3(8), 124.0(5), and 125.7(5)°, respectively, give some indication of the internal strain within the dinuclear cation.

Twisting of the metal co-ordination planes results in the formation of relatively high torsional (dihedral) angles around the C–C bonds in both five-membered chelate rings. These angles obtained for N(1)–C(6)–C(7)–N(2) and N(3)–C(16)–C(17)–N(4) are −34.2 and −33.8°, respectively. Since it is not unreasonable that these torsional angles are retained in solution (see above), their high value may effectively slow down the pseudo-rotation of these fragments.

Finally, for completeness, an illustration of the packing of dinuclear units in the solid state is given in Figure 4. The shortest non-bonded distances to Ni(1) and Ni(2) are 3.46 and 3.56 Å, and are associated with the C(3) and N(4) atoms of neighbouring molecules, respectively. The Ni(1) • • • Ni(1) and Ni(2) • • • Ni(2) distances are 4.45 and 3.66 Å, respectively, and indicate that the packing forces are predominantly van der Waals in nature.

Experimental

Materials.—7-Amino-4-methyl-5-azahept-3-en-2-one (**2**), 4-chloro-2,6-diformylphenol (**4a**), and 2,6-diformyl-4-methylphenol (**4b**) were prepared according to the literature procedures.[1,6,7] All other chemicals were reagent grade and were used without further purification.

[4-*Chloro*-2-*formyl*-6-(4-*methyl*-2-*oxo*-5,8-*diazanona*-3,8-*dienyl*)*phenolato*(2−)]*nickel*(II) (**7a**).—To a vigorously stirred solution of compound (**4a**) (0.92 g, 5 mmol) in dichloromethane (40 cm^3) was added dropwise, a solution containing (**2**) (0.71 g, 5 mmol) in dichloromethane (20 cm^3). The mixture was stirred for 30 min at room temperature and then filtered through 4A molecular sieves to remove water formed in the reaction. The solvent was evaporated and the oily residue extracted repeatedly with hot hexane. Upon cooling the extracts yielded a crude Schiff-base ligand, 4-chloro-2-formyl-6-(4-methyl-2-oxo-5,8-diazanona-3,8-dienyl)phenol (**5a**) [M^+, m/z 308 (100%) in f.d. mass spectrum] in the form of a yellow powder (1.26 g).

Table 5. Structure determination summary for the dinuclear nickel complex (**8a**)

Crystal data	
Empirical formula	$C_{44}H_{54}Br_2Cl_2N_8Ni_4O_7$ (= 2 molecules)
Colour and habit	Red multifaceted needles
Size/mm	0.10 × 0.12 × 0.40
Space group	$C2/c$ (no. 15)
Unit-cell dimensions	a = 22.082(4), b = 11.511(1), c = 22.368(4) Å, β = 118.61(1)°
U/Å^3	4 991(1)
Z	8 Molecules per cell
D_c, D_m/g cm^{-3}	1.69, 1.69[a]
F(000)	2 584
Data collection	
Radiation	Mo-K_α (λ 0.71073 Å)
Monochromator	Highly oriented graphite crystal
Temperature	Ambient (294 K)
hkl Limits	±25, +14, +25
Scan range	0.8 on either side of $K_{\alpha 12}$
Background measurement	Stationary crystal and counter at beginning and end of scan, total background-to-scan time ratio of 0.5:1
μ(Mo-K_α)/cm^{-1}	31.96
No. of φ-scan reflections	5
Refinement	
System used	MicroVAX II, Nicolet SHELXS/SHELXTL PLUS
Solution	Direct methods (TREF)
Final residuals	R = 0.0380, R' = 0.0318[b]
Goodness of fit	S = 1.21[c]
Largest |shift/e.s.d.|	0.001
Number of variables	318
Data-to-parameter ratio	5.0:1
Max./min. excursions	0.39 and −0.40 e Å^{-3}

[a] By flotation in 1,1,1-trichloroethane–1,2-dibromoethane. [b] $R = \Sigma(||F_o| - |F_c||)/\Sigma|F_o|$, $R' = [\Sigma(w||F_o| - |F_c||^2)/\Sigma w|F_o|^2]^{\frac{1}{2}}$, $w = [\sigma^2(F) + |g|F^2]^{-1}$, g = 0.000 100. [c] $S = [\Sigma(w||F_o| - |F_c||^2)/(M - N)]^{\frac{1}{2}}$ where M is the number of observed reflections and N the number of parameters refined.

This material (1.04 g, *ca.* 3.4 mmol) was dissolved in methanol (20 cm^3) and combined with a solution of nickel acetate tetrahydrate (0.84 g, 3.4 mmol) in methanol (30 cm^3). After stirring for 30 min at room temperature the mixture yielded a red-brown precipitate which was filtered off, washed with cold methanol, and recrystallized from dichloromethane to give the nickel complex (**7a**) as fine red-brown needles (0.97 g), m.p. 287 °C (Found: C, 49.3; H, 4.2; N, 7.8. $C_{15}H_{15}ClN_2NiO_3$ requires C, 49.3; H, 4.1; N, 7.7%).

[2-*Formyl*-4-*methyl*-6-(4-*methyl*-2-*oxo*-5,8-*diazanona*-3,8-*dienyl*)*phenolato*(2−)]*nickel*(II) (**7b**).—The ligand 2-formyl-4-methyl-6-(4-methyl-2-oxo-5,8-diazanona-3,8-dienyl)phenol (**5b**) was prepared similarly to (**5a**) and isolated as a yellow powder (1.16 g) by extraction of the product formed in the reaction of (**4b**) (0.82 g, 5 mmol) and (**2**) (0.71 g, 5 mmol) with hot di-isopropyl ether [M^+, m/z 288 (100%) in f.d. mass spectrum of the ligand]. The reaction of (**5b**) (0.98 g, 3.4 mmol) with nickel acetate was carried out as in the case of (**5a**), and the nickel complex was recrystallized from methanol to give 0.86 g (**7b**) as fine red-brown crystals, m.p. 235 °C (Found: C, 55.5; H, 5.2; N, 8.2. $C_{16}H_{18}N_2NiO_3$ requires C, 55.7; H, 5.3; N, 8.1%).

[4-*Chloro*-2,6-*bis*(4-*methyl*-2-*oxo*-5,8-*diazanona*-3,8-*dienyl*)*phenolato*(3−)]*dinickel*(II) *Bromide Hemihydrate* (**8a**).—A solution of compound (**4a**) (0.92 g, 5 mmol) and (**2**) (1.42 g, 10 mmol) in dichloromethane (50 cm^3) was refluxed for 1 h, then cooled to room temperature and filtered through A4 molecular sieves. The filtrate was concentrated under reduced pressure and the ligand extracted from the residue with hot hexane. Upon cooling the hexane extracts yielded the crude ligand 4-chloro-2,6-bis-(4-methyl-2-oxo-5,8-diazanona-3,8-dienyl)phenol (**6a**) [M^+, m/z 432 (100%) in f.d. mass spectrum] as a yellow solid (1.77 g). A solution of nickel bromide trihydrate (1.36 g, 5 mmol) in methanol (25 cm^3) was combined with a solution of (**6a**) (1.10 g, 2.5 mmol) and triethylamine (0.76 g, 7.5 mmol) in methanol (20 cm^3) and the mixture stirred for 30 min at room temperature. Then the brown solution was concentrated to half its volume and after several hours a brown precipitate formed. The precipitate was recrystallized from methanol to give 0.63 g of the nickel complex (**8a**) as brown prisms (Found: C, 41.6; H, 4.3; N, 9.0. $C_{22}H_{27}BrClN_4Ni_2O_{3.5}$ requires C, 41.5; H, 4.3; N, 8.8%).

[4-*Methyl*-2,6-*bis*(4-*methyl*-2-*oxo*-5,8-*diazanona*-3,8-*dienyl*)-*phenolato*(3−)]*dinickel*(II) *Bromide Hemihydrate* (**8b**).—The ligand 4-methyl-2,6-bis(4-methyl-2-oxo-5,8-diazanona-3,8-dienyl)phenol (**6b**) was prepared as for (**6a**) and isolated as an orange-yellow solid by extraction of the crude product formed in the reaction between (**4b**) (0.82 g, 5 mmol) and (**2**) (1.42 g, 10 mmol) with hot di-isopropyl ether [M^+, m/z 412 (100%) in f.d. mass spectrum of the ligand]. The complexation with nickel(II) was carried out as in the case of (**6a**) but with (**6b**) (1.03 g, 2.5 mmol), and the resulting complex was recrystallized from methanol to give 0.84 g of (**8b**) as a brown microcrystalline solid (Found: C, 44.9; H, 5.1; N, 9.0. $C_{23}H_{30}BrN_4Ni_2O_{3.5}$ requires C, 44.9; H, 4.9; N, 9.1%).

Physical Measurements.—Elemental analyses were performed on a Carlo Erba MOD 1106 elemental analyzer. Field desorption mass spectra of the ligands were recorded on a Varian Mat 711 spectrometer with accelerating voltage 8 kV, extracting voltage −3 kV, and emitter current 10 mA. Fast atom bombardment mass spectra of the nickel complexes were recorded using *m*-nitrobenzyl alcohol as a matrix on a VG 30-250 spectrometer (VG Instruments Inc.) at the probe temperature; xenon was used as the primary beam gas and the ion gun was operated at 8 kV and 100 μA. Proton and ^{13}C n.m.r. spectra were run on a 300-MHz Nicolet spectrometer in $CDCl_3$ solution with $SiMe_4$ as internal reference. U.v.–visible spectra were recorded on a Perkin-Elmer 402 spectrometer in methanol solution, and i.r. spectra (1 500—4 000 cm^{-1} region) on a Perkin-Elmer 621 spectrometer in Nujol and/or hexachlorobutadiene mulls.

X-*Ray Crystallography of Complex* (**8a**).—The crystals of the complex (**8a**) for *X*-ray structure determination were grown by slow infusion of di-isopropyl ether into a chloroform solution of the complex. A suitable crystal was mounted on a glass fibre with epoxy cement and transferred to a Nicolet R3m four-circle diffractometer for characterization and data collection. Unit-cell parameters were determined from the angular settings of 25 well centred reflections (21 < 2θ < 31). Axial photographs, and a limited search through an octant of reciprocal space, revealed systematic absences and symmetry consistent with the monoclinic space group $C2/c$ (no. 15). Crystal data are summarized in Table 5.

Data collection parameters are given in Table 5. The θ—2θ scans were collected with variable scan speeds from 2.0 to 29.3° min^{-1}. One quadrant of data (±h, +k, +l) was collected with 2θ ranging from 3.0 to 45.0°. A total of 3 596 reflections were measured and corrected for Lorentz-polarization and absorption effects (empirical correction based on five azimuthal reflections with 11 < 2θ < 30° and 279 < χ < 285°; minimum and maximum transmission factors 0.703 and 0.784, respec-

tively). Three standard reflections were remeasured every 37 reflections as a means of monitoring instrument and crystal stability during the course of the experiment. The intensities of those standards showed a random drift or variation ranging from 0.9640 to 1.0114 with no observable decomposition in the sample. A correction curve was used to scale the general data to account for the observed drift. Data processing yielded 3 293 unique reflections of which 1 576 had $F > 6\sigma(F)$ with $R_{int.} = 0.0201$ for the averaging of equivalent reflections.

The structure was successfully solved in the monoclinic space group $C2/c$ (no. 15), and refined by full-matrix least squares. A combination of direct methods (SHELXS with the TREF option[8]) and Fourier techniques was used to locate the positions of the non-hydrogen atoms. The refinement of this model with absorption-corrected data and a weighting scheme based on $\sigma(F)$ yielded $R = 0.0497$ and $R' = 0.0638$. Hydrogen parameters were then introduced as follows: (*a*) the crystallographically independent H atom for the water of hydration was located in a Fourier-difference map and its co-ordinates allowed to refine; (*b*) a riding model was used for the remaining H atoms with C–H 0.96 Å; (*c*) the methyl moieties were refined as rigid groups with rotational freedom; (*d*) all of the H atoms were assigned fixed isotropic values of $U_H = 0.08$ Å^2. The structure converged to $R' = 0.0318$. The final values for the refinement indices are given in Table 5 and fractional atomic co-ordinates are in Table 2.

Additional material available from the Cambridge Crystallographic Data Centre comprises H-atom co-ordinates, thermal parameters, and remaining bond distances and angles.

Acknowledgements

This research was supported by Grant CPBP.01.12 from the Polish Academy of Sciences, Grant No. 21276 from the National Institutes of Health (to E. D.), and by Instrumentation Grant CHE 8102974 from the National Science Foundation.

References

1 E. Kwiatkowski and M. Kwiatkowski, *Inorg. Chim. Acta*, 1984, **82**, 101.
2 J. P. Costes, G. Cros, M. H. Darbieu, and J. P. Laurent, *Inorg. Chim. Acta*, 1982, **60**, 111; J. P. Costes, *ibid.*, 1987, **130**, 17; R. C. Coombes, J. P. Costes, D. E. Fenton, *ibid.*, 1983, **77**, L173; J. P. Costes and M. I. Fernandez-Garcia, *Transition Met. Chem.*, 1988, **13**, 131; T. Nagahara, M. Suzuki, and K. Kasuga, *Inorg. Chim. Acta*, 1988, **149**, 279.
3 E. Kwiatkowski and M. Kwiatkowski, *Inorg. Chim. Acta*, 1986, **117**, 145.
4 L. Sacconi, P. Nannelli, and U. Campigli, *Inorg. Chem.*, 1965, **4**, 818.
5 See, for example, R. P. Scaringe and D. J. Hodgson, *Inorg. Chem.*, 1976, **15**, 1193; L. L. Lindoy, W. E. Moody, and D. Taylor, *ibid.*, 1977, **16**, 1962; K. A. Goldsby, A. J. Jircitano, D. M. Minahan, D. Ramprasad, and D. H. Busch, *ibid.*, 1987, **26**, 2651; F. Cariati, F. Morrazoni, C. Busetto, G. D. Piero, and A. Zazzetta, *J. Chem. Soc., Dalton Trans.*, 1976, 342; T. F. Lai, S. F. Tan, K. P. Ang, and T. C. W. Mak, *Transition Met. Chem. (Weinheim, Ger.,)* 1985, **10**, 375; A. Mederos, A. Medina, E. Medina, F. G. Manrique, P. Nunez, and M. Rodriguez, *J. Coord. Chem.*, 1987, **15**, 393.
6 A. Kinke, F. Harnus, and E. Ziegler, *J. Prakt. Chem.*, 1939, **152**, 126.
7 F. Ullman and K. Brittner, *Chem. Ber.*, 1909, **42**, 2539.
8 G. M. Sheldrick in 'Crystallographic Computing,' eds. G. M. Sheldrick, C. Kruger, and R. Goddard, Oxford University Press, 1985, vol. 3, pp. 175–189.

Received 20*th December* 1989; *Paper* 9/05418I